AUTHOR(S): MADDAHI, Y., LIAO, S., FUNG, W.-K. and SEPEHRI, N.

TITLE: Position referenced force augmentation in teleoperated hydraulic manipulators operating under delayed and lossy networks: a pilot study.

YEAR: 2016

Accepted Manuscript

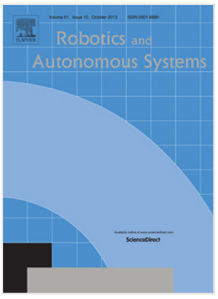

Position referenced force augmentation in teleoperated hydraulic manipulators operating under delayed and lossy networks: A pilot study

Yaser Maddahi, Stephen Liao, Wai-keung Fung, Nariman Sepehri

PII: S0921-8890(16)30204-4
DOI: http://dx.doi.org/10.1016/j.robot.2016.04.006
Reference: ROBOT 2626

To appear in: *Robotics and Autonomous Systems*

Received date: 4 June 2014
Revised date: 24 November 2015
Accepted date: 12 April 2016

Please cite this article as: Y. Maddahi, S. Liao, W.-k. Fung, N. Sepehri, Position referenced force augmentation in teleoperated hydraulic manipulators operating under delayed and lossy networks: A pilot study, *Robotics and Autonomous Systems* (2016), http://dx.doi.org/10.1016/j.robot.2016.04.006

Position referenced force augmentation in teleoperated hydraulic manipulators operating under delayed and lossy networks: A pilot study

Yaser Maddahi[1], Stephen Liao[2], Wai-keung Fung[3] and Nariman Sepehri[1]

[1] Department of Mechanical Engineering, University of Manitoba, Winnipeg, MB, Canada.
[2] Department of Electrical and Computer Engineering, University of Manitoba, Winnipeg, MB, Canada.
[3] School of Engineering, Robert Gordon University, Aberdeen, United Kingdom.

Corresponding author: Nariman.Sepehri@umanitoba.ca

ABSTRACT: Position error between motions of the master and slave end-effectors is inevitable as it originates from hard-to-avoid imperfections in controller design and model uncertainty. Moreover, when a slave manipulator is controlled through a delayed and lossy communication channel, the error between the desired motion originating from the master device and the actual movement of the slave manipulator end-effector is further exacerbated. This paper introduces a force feedback scheme to alleviate this problem by simply guiding the operator to slow down the haptic device motion and, in turn, allows the slave manipulator to follow the desired trajectory closely. Using this scheme, the master haptic device generates a force, which is proportional to the position error at the slave end-effector, and opposite to the operator's intended motion at the master site. Indeed, this force is a signal or cue to the operator for reducing the hand speed when position error, due to delayed and lossy network, appears at the slave site. Effectiveness of the proposed scheme is validated by performing experiments on a hydraulic telemanipulator setup developed for performing live-line maintenance. Experiments are conducted when the system operates under both dedicated and wireless networks. Results show that the scheme performs well in reducing the position error between the haptic device and the slave end-effector. Specifically, by utilizing the proposed force, the mean position error, for the case presented here, reduces by at least 92% as compared to the condition without the proposed force augmentation scheme. The scheme is easy to implement, as the only required on-line measurement is the angular displacement of the slave manipulator joints.

KEYWORDS: Position error-referenced force; haptics; hydraulic manipulator; teleoperation; wireless network; dedicated network; time delay; packet loss.

1. INTRODUCTION

A teleoperated system is composed of a master site where a human operator utilizes a hand-controller to guide a remote robot, a slave site in which a manipulator follows the behaviour of the hand-controller, and a communication channel that connects both the slave and master sites. Ideally, the slave manipulator should exactly follow the scaled master motion, *i.e.*, there should be no error between the position of the master and the position of the slave end-effector. In practice, however, the position error at the slave manipulator occurs due to many reasons such as lack of responsiveness in controller or actuation system, and coupled dynamics. Moreover, when the teleoperated system operates under a delayed and lossy network, the information, transmitted between the operator and the slave, can be delayed or lost. This further contributes to the position error at the slave end-effector. Network delay refers to the time it takes for a packet of data to travel across the network from a source node to a destination node. Network delays in a communication channel are caused by the time: (*i*) required to process packet headers, (*ii*) spent in routing queues, (*iii*) needed to push packet bits into the physical link, and (*iv*) required for a signal to reach its destination via the link[1]. Packet loss occurs when one or multiple data packets fail to reach a destination. This is caused by channel congestion, data rejection in-transit, faulty network drivers, or signal attenuation[2]. Network disturbances, such as environmental obstruction, also affect the packet loss in a wireless channel.

One method to decrease the position error is to predict the delays and losses in the communication channel, and then apply the predicted variables to the control system[3-6]. Examples are wave variable based controllers[7,8] that provide stable bilateral control of teleoperated systems. Tanner and Niemeyer[9] introduced the concept of reflection shaping through wave filters to mitigate undesirable aspects of wave reflections. They further implemented their technique to contact control with hard environments and in the presence of time delay[10]. There exist several limited studies focusing on increasing transparency between the master and slave manipulators[11-18]. For example, problem of improving transparency during performance of contact tasks under a delayed communication channel was addressed by Secchi *et al.*[11] and Arcara and Melchiorri[12]. A bilateral control strategy that passively compensated transparency when transitioning between free motion and hard contact motion scenarios was proposed by Rodriguez-Seda[13].

Another method to reduce the position error at the slave end-effector is to signal the operator to correct their hand motion accordingly. A haptic force is generated as an indicator to any task trajectory deviation[19,20]. This haptic force can be built upon the position error between the slave end-effector and the master (slave position error-referenced force)[21]. Sankaranarayana and Hannaford[22,23] presented variations of this concept that allow two operators cooperatively move a box along a direction in a networked haptic virtual environment. Kontz *et al.*[24] proposed a scheme commanding the haptic device to generate a force that synchronizes the motion of a haptic device to the excavator bucket movement. Hayn and Schwarzmann[25] implemented a scheme similar to the Kontz *et al.*[25] for teleoperation of a hydraulic excavator. Ahn *et al.*[26] proposed a compliance control scheme for a position-referenced bilateral system in which the position difference between master and slave sites is treated as an equivalent contact force. In all of the above studies, positions of the haptic device (master) and the manipulator (slave) provide a position error vector for the haptic force (hereafter, called conventional haptic force) augmentation in teleoperation control. The conventional haptic force is then generated parallel to, and in proportion with, the magnitude of the position error vector at the slave end-effector. The conventional force indicates to the operator whether the slave manipulator is moving ahead or behind the intended desired trajectory. Although the conventional force provides information about the magnitude of the position error, the information contained in its direction is not adequate to effectively reduce the position error. Specifically, this conventional force does not serve to slow down the operator hand's motion for the slave manipulator to catch up commands sent by the master device through a delayed/lossy channel.

In order to effectively alleviate the effect of position errors at the slave end-effector, we propose to modify the slave position error-referenced force to always be in the opposite direction of the operator's hand current velocity. The intention is to slow down the operator's hand motion that results in better coordination between the master device and the slave manipulator. Reducing the speed gives the slave manipulator an opportunity to move closer to its desired trajectory. The proposed force therefore signals the operator to slow down the motion. In particular, while the operator cannot accurately perceive the position error, due to network delay and packet loss, the force allows them to stay alert of the extent the hydraulic manipulator lags behind the haptic device. As compared to the conventional scheme whereby the direction of the force is parallel to the slave position error[21-26], in our proposed scheme, the force direction is always opposite to the

direction of the operator's hand motion. This paper presents a pilot study that validates the effectiveness of the scheme for a telemanipulation platform that is used to conduct a typical live-line maintenance task using a hydraulic manipulator controlled through both a dedicated line (with constant delay and packet loss) and a wireless network (with time-varying delays and packet losses). Empirical results, presented in this paper, demonstrate improvement of position error in manipulation tasks by our proposed scheme as compared to the conventional scheme under a wide range of network scenarios. The proposed force augmentation scheme can be easily ported to other telemanipulation platforms for testing.

It is worth mentioning that the proposed force scheme should not be mistaken with the impedance-type virtual fixture scheme[27-29]. In an impedance-type virtual fixture scheme, the haptic force is proportional to the difference between the actual and desired positions at the slave end-effector, and its direction is orthogonal to the intended trajectory of the haptic device[30-32]. No information about the position of the slave is used in virtual fixture scheme. The authors have shown that augmenting virtual fixture forces by the proposed method mitigates the position errors between master and slave robots[33]. They combined virtual fixture and augmentation force to reduce position errors at both master device and the slave manipulator[33]. Specifically, in the proposed scheme, slave desired trajectory is produced in real-time by the operator. The slave robot will therefore follow the intended trajectory under the influence of the lossy and delayed communication channel.

The rest of this paper is organized as follows. The proposed force feedback system is described in Section 2. Section 3 presents an overview of the experimental setup including the hydraulic telemanipulator and the network simulator. Section 4 presents the test procedure and experimental methodology used to validate the proposed scheme. Experimental results are shown in Section 5. Section 6 outlines the conclusions of this paper.

2. SLAVE POSITION ERROR-REFERENCED FORCE SCHEME

2.1. Proposed approach

Figure 1 illustrates how the haptic force, applied to the operator's hand, is produced. The desired (P_s^d) and actual (P_s^a) positions of end-effector are denoted by (x^d, y^d, z^d) and (x^a, y^a, z^a), respectively. The position error vector (E) of the slave end-effector is defined by (see Figure 1a):

$$E = \begin{pmatrix} e_x \\ e_y \\ e_z \end{pmatrix} = \begin{pmatrix} x^a - x^d \\ y^a - y^d \\ z^a - z^d \end{pmatrix} \quad (1)$$

Note that the desired position of the slave end-effector is obtained from the scaled position of the haptic device implement. The proposed position error-referenced force, F_{PR}^{p}, is computed by multiplying the position error vector by an impedance matrix (G) while the force, applied to the hand, is opposite in direction to the current velocity of the haptic device, $\hat{v}$:

$$F_{PR}^{p} = \begin{cases} -\|G(E - E_{thr})\| & \|E\| > \|E_{thr}\| \\ 0 & \|E\| \leq \|E_{thr}\| \end{cases} \quad (2)$$

In (2), the impedance matrix is defined by $G = diag[k_x\ k_y\ k_z]$. Note that k_x, k_y and k_z represent the ability of the scheme in providing different levels of force compliance along x_R, y_R, z_R axes, respectively. For instance, by decreasing the value of k_x, the operator has more freedom to move along x_R axis. Note that this force is only generated when the position error is greater than a threshold. In other words, when $\|E\| \leq \|E_{thr}\|$, the haptic device does not produce any haptic force. When $\|E\| > \|E_{thr}\|$, the magnitude of $\vec{F}_{PR}^{p}$ is proportional to $|E - E_{thr}|$. The threshold reflects the manipulator controller accuracy, and is considered to prevent unnecessary force activation. The negative sign indicates that the haptic force is opposite to the direction of the operator's hand motion (see Figure 1b). The instantaneous velocity, $\hat{v}$, is directly read from the haptic device through designated Application Programming Interface (API) of the haptic device.

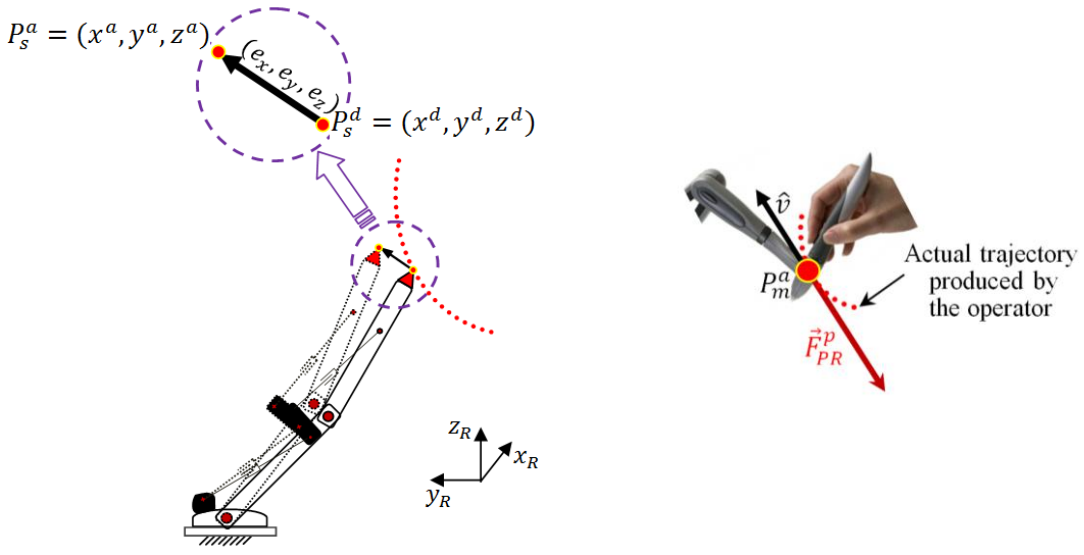

(a) (b)

Figure 1. (a) position error at the slave end-effector described in frame $\{x_R y_R z_R\}$; (b) unit vector of operator's hand velocity ($\hat{v}$) and haptic force (F_{PR}^{p}).

Figure 2 shows the block diagram of the proposed scheme. As observed, the operator moves the haptic device end-effector. Then, the actual position of the haptic device, *i.e.*, the actual position of the operator's hand (P_m^a), is multiplied by k_s (scaling factor) in order to find the desired position of the manipulator end-effector, P_s^d. The desired position is then sent to the slave site through a communication channel. The actual position of the slave manipulator end-effector, P_s^a, is computed by forward kinematics of the slave manipulator using the measured angular displacements of the slave joints (θ_s^a)[34]. The controller is a PI controller that is augmented by dead-band and braking acceleration-based compensation to reduce the effects of dead-band and dry friction[35]. The slave manipulator controller utilizes the angular displacement error ($\theta_s^a - \theta_s^d$) to generate the control signal (u) for the hydraulic valves. The difference between the actual and the desired positions of the slave end-effector ($P_s^a - P_s^d$) gives the position error at the end-effector (E), which is then used to find the position error-referenced force (F_{PR}^p). The magnitude of the haptic force indicates how the operator needs to move the haptic device slower until no force is perceived.

Note that the master site receives delayed or lossy information of the slave site. However, both force and position error are determined at the master side in which the local delay is zero and there is only a very small amount of processing delay. Therefore, there is no delay between the force calculated and position error received by the master computer.

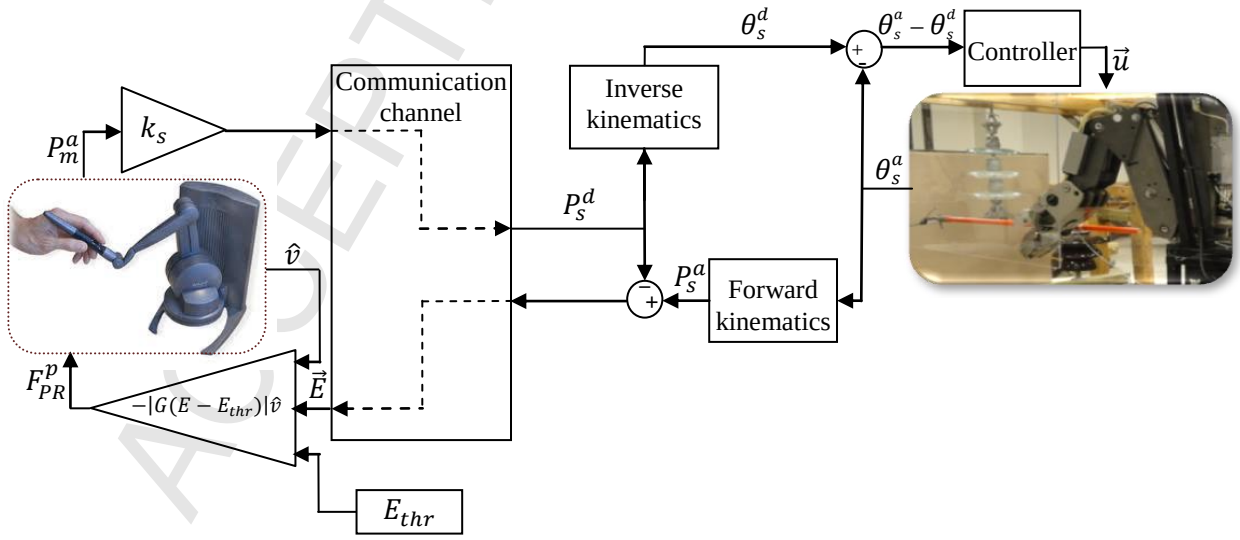

Figure 2. Block diagram of the proposed position error-referenced force scheme.

2.2. *Comparing proposed and conventional position-referenced force schemes*

Figure 3 illustrates a graphical interpretation of two proposed and conventional schemes. Figure 3a shows four typical position errors at the slave end-effector at points A ($E^s_{e,1}$), B ($E^s_{e,2}$), C ($E^s_{e,3}$) and D ($E^s_{e,4}$). Figure 3b illustrates the direction of the conventional haptic force (F^c_{PR}) which is parallel to the vector of position error at the slave side (E^s_e). As observed, the conventional force is not applied opposite to the operator's hand motion (hand speed or haptic device speed). Thus, this force does not serve to signal the operator to slow down their hand motion, as it is difficult for the operator to analyze and differentiate components of the applied for during performance of a task. As seen in Figure 3c, the proposed force (F^p_{PR}) is applied in a direction same as the haptic device current velocity (the operator's hand current velocity). Therefore, when the operator moves fast, which results in discoordination between the master and the slave, a force is applied to the operator's hand against the direction of motion. The applied force therefore is used as a signal for slowing down the motion.

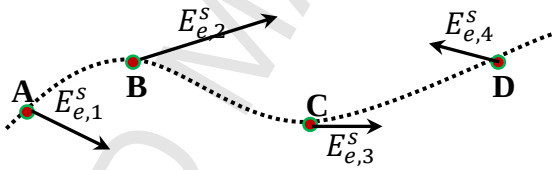

(a) Vector of position error at slave end-effector when the haptic device passes points A to D ($\vec{E}^s_{e,1}$ to $\vec{E}^s_{e,4}$)

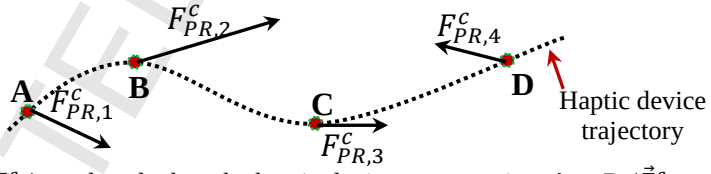

(b) Conventional force (F^c_{PR}) produced when the haptic device passes points A to D ($\vec{F}^c_{PR,1}$ to $\vec{F}^c_{PR,4}$)

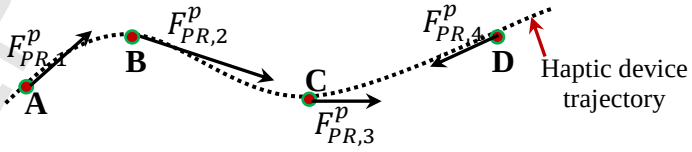

(c) Proposed force (F^p_{PR}) produced when the haptic device passes points A to D ($\vec{F}^p_{PR,1}$ to $\vec{F}^p_{PR,4}$)

Figure 3. Graphical interpretation of proposed position referenced force scheme and conventional scheme. In proposed scheme, the haptic force (F^p_{PR}) is always parallel to trajectory of the haptic device, while the conventional force (F^c_{PR}) is always parallel to the position error at the slave end-effector (E^s_e).

3. EXPERIMENTAL SETUP

3.1. *System architecture*

Figure 4 illustrates the general architecture of the experimental hydraulic telemanipulator platform consisting of a haptic device (master) guided by an operator, and a hydraulic

manipulator (slave). As shown in Figure 4, the master and slave sites are connected through a communication channel. Three PCs are located at the master, slave, and communication channel stations, respectively. The computers are connected in a local area network (LAN) through an Ethernet hub. User Datagram Protocol (UDP) is chosen as the transport protocol. Therefore, there is no delay from waiting for packet acknowledgements and retransmissions. The intermediate computer runs the Network Simulator Version 2 (NS2) which generates various network scenarios based on controllable parameters of the communication channel such as time delay and packet loss[36]. Using the NS2, consistent and controlled conditions can be provided for the communication link, and the experiment can be performed under specific network protocols and topologies. In our designed experiments, the NS2 emulates both the dedicated network (with constant packet loss and near-constant latency) and the wireless network (with time-varying time delay and packet loss).

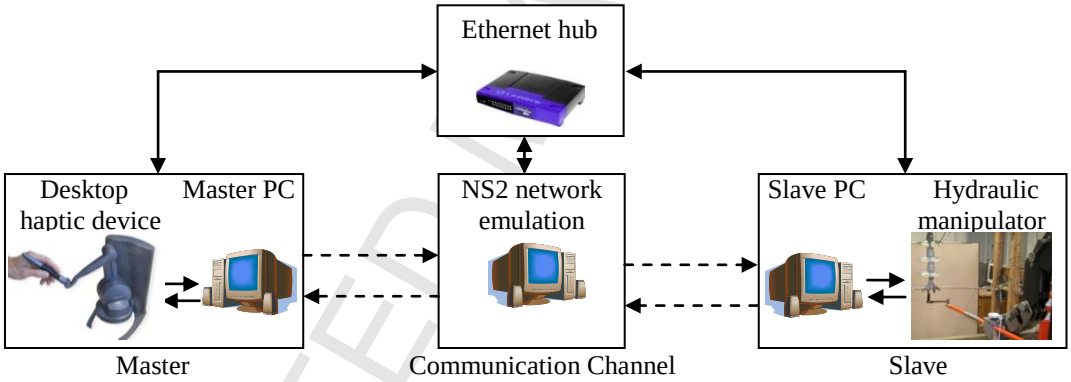

Figure 4. General architecture of the teleoperated hydraulic manipulator. Solid and dashed lines show physical and logical connections, respectively.

3.2. Master-slave setup

Figure 5 shows the test rig comprising a slave Kodiak hydraulic manipulator, and a master PHANToM Desktop haptic device. This test rig is part of an experimental platform to perform live-line maintenance tasks. The master and slave devices are connected to PCs using parallel port and data acquisition boards, respectively. The data acquisition boards are used to send control signals to the servovalves, and read the angular displacement of manipulator joints measured by Hall Effect sensors[34]. Displacements are then substituted into forward kinematic equations to calculate the current position and orientation of the tool located at the slave end-effector. The information is then forwarded to the master site through the communication channel. The nonlinear PI (NPI) controller[35] was used on the slave manipulator. The NPI (i) has

excellent tracking and regulating ability, (*ii*) responds quickly to variations of the set point, (*iii*) reverses the directions quickly without overshoot, and (*iv*) retains the above properties for both large and small changes in the set point[35]. The NPI controller was shown to improve tracking accuracy by a factor of five, as compared to the conventional PI controller with fixed gains, without sacrificing regulation accuracy or robustness. The accuracy of the NPI controller is about 0.2 degree[39]. This controller produced a steady-state error (E_{thr}) of 1.54 mm 1.06 mm and 2.07 mm at the slave end-effector along x_R, y_R and z_R axes, respectively. The steady-state error was determined by moving the robot along a desired trajectory autonomously and under different low speeds.

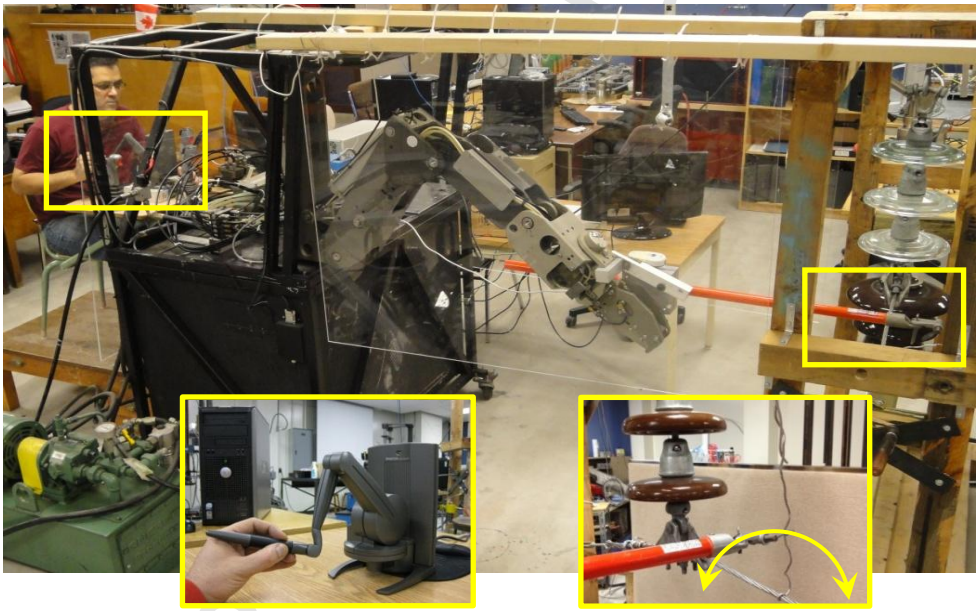

Figure 5. Teleoperation test rig: master haptic device and slave hydraulic manipulator. Arrow shows the semicircular path defined to twist tie wire around an electrical cable.

3.3. Communication channel

The NS2 is a common simulator for studying the behaviour of computer networks, and allows users to generate simulation scenarios with different protocols and topologies for both dedicated and wireless networks[36]. The NS2 was employed in our experiments for its availability, widespread use, and ability to be extended[36]. When the NS2 runs under network emulation mode, it captures an incoming packet, and then injects it into the simulation in real-time. The packet is delayed or dropped according to the defined network scenarios. After the packet is delayed, it is forwarded to the slave site by the network emulator.

In the setup, the master and slave are able to transmit data packets in a continuous fashion. Both the master and slave are set to send packets to the emulator. The emulator changes the source and destination addresses of any incoming packets. Thus, the network emulator controls when packets are received by the master and slave computers. To ensure that the experiment can be repeated multiple times with the same network conditions, the network simulation clock is synchronized with the time of the master and slave.

The NS2 is also employed to simulate wireless networks under simple obstruction models and different transmission power of router antenna[36]. Using NS2, the simulation of wireless networks is performed by specifying the radio propagation model, the medium access control (MAC) layer protocol, and the ad hoc routing protocol.

In practice, the surrounding environment clutter may vary vastly between the master and slave sites. Therefore, the received power is represented as a random variable and distributed in log-normal distribution (normal distribution in dB) at any distance of d. In wireless communication systems, a target minimum received power level (P_{min}) is defined, below which performance of the teleoperated system becomes unacceptable, *i.e.*, the system exhibits instability and/or poor transparency. The probability of dropping a packet (*i.e.*, the received signal level is below P_{min} or the amount of packet loss in the wireless communication channel) is given as follows[37],

$$prob[P_r(d)]_{dB} = prob\left[[P_r(d_0)]_{dB} - 10nlog\left(\frac{d}{d_0}\right) + X_\sigma \leq [P_{min}]_{dB}\right] \qquad (3)$$

where the power received by the receiver antenna is denoted by P_r. d_0 is the reference distance. $P_r(d_0)$ denotes the received power for a given d_0[37]. X_σ represents a Gaussian random variable with zero mean value, and standard (shadowing) deviation σ (in dB). Note that the characteristic of the environment obstruction is introduced using σ and n (the path loss exponent). Empirical measurements of coefficients n and σ, for a number of wave propagation cases, are found in literature[34]. For example, the values of n and σ are 2 dB and 4 dB respectively, for an outdoor environment without any obstacle.

4. TEST PROCEDURE

Experiments were set up to investigate how effectively the proposed scheme reduces the position error at the slave hydraulic manipulator, shown in Figure 5, when it is controlled through dedicated or wireless networks. Experiments were conducted when the force capability

of the haptic device was deactivated (force-disabled mode), and then similarly repeated when the position error-referenced force was generated by the haptic device (force-enabled mode). The evaluation criterion was the position error at the slave manipulator end-effector. However, in addition to position error, the average of the mean values of operator's hand speeds and task completion times were reported. In the experiments, the stability of the entire teleoperated control system was investigated by visually observing if the oscillations in the responses are bounded[2,20].

Participants were asked to move the haptic device along a semicircular trajectory, which resulted in guiding the hydraulic manipulator end-effector along the trajectory shown in Figure 6. This trajectory emulates the task of twisting the tie wire around an electrical cable, in live-line maintenance (see Figure 5). For each participant, a one-week training period (30 minutes a day) was provided to familiarize them about the operation of the entire system before starting the experiments. Robot-assisted live-line maintenance procedure was designed for several tasks, and was documented under supervision of an expert from Manitoba Hydro. All participants went through the same learning procedure. The training was continued until the operator felt comfortable using the haptic hand-controller and performing live-line maintenance tasks.

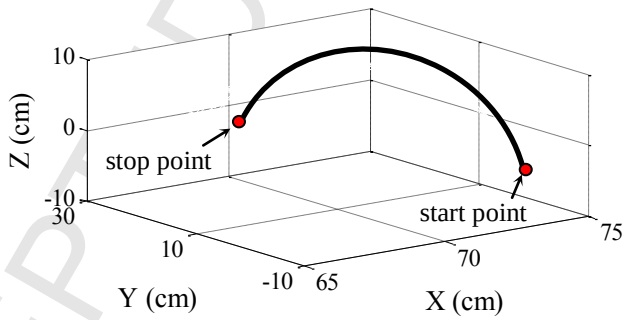

Figure 6. Desired trajectory of hydraulic manipulator end-effector defined for validation tests.

For each force mode, five participants conducted ten trial runs. In total, 20(scenarios) ×10(trials) ×2(schemes) = 400 trials were performed by each operator: 16 scenarios under dedicated networks, and 4 scenarios under wireless communication channels. The wireless network was configured according to different combinations of obstructions in the environment and antenna transmission powers. Each test was repeated 10 times by the same operator and performed with or without force feedback, while the operator utilized direct visualization to control the situation of conducting the task. The operator was blinded from the aims and

hypotheses of the study, and was not informed whether the performance of the task is with the proposed scheme (force-enabled) or without proposed scheme (force-disabled). The operator was also not informed about how he/she performed in each trial. Although the operator was asked to repeat the same movement in each trial, deviations from trajectories were unavoidable.

5. RESULTS

5.1. Validation under dedicated channels

In the first set of experiments, the system was examined under dedicated communication channels configured at different pairs of constant time delays and constant packet losses. In haptic force-enabled trials, the haptic force was generated based on the position error at the slave end-effector. The operator was instructed to reduce the hand speed, upon sensing the haptic force, with the intention of minimizing the force. In total, 320 trial runs were conducted with and without force, each with four constant time delays (400 ms, 700 ms, 1000 ms and 1300 ms) and four constant packet losses (0%, 25%, 50% and 75%). There was an inherent 400 ms delay originating from the processing time of the master and slave computers. The value of 400 ms was obtained by directly connecting the master and slave PCs, without introducing any time delay in the communication channel. Table 1 summarizes the test scenarios.

Table 1. Characteristics of dedicated networks used in first set of experiments.

	Test number															
	S1	S2	S3	S4	S5	S6	S7	S8	S9	S10	S11	S12	S13	S14	S15	S16
Round-trip delay, TD (ms)	400				700				1000				1300			
Packet loss, PL (%)	0	25	50	75	0	25	50	75	0	25	50	75	0	25	50	75

In all experiments, the impedance matrix (G) was set to $diag[250\frac{N}{m}\ 250\frac{N}{m}\ 250\frac{N}{m}]$. The gains were chosen to produce a feeling of an unsaturated force, when the time delay and packet loss were set to 400 ms and 0%, respectively. The PHANToM Desktop haptic device has limitation in producing force up to 7.9 N which means that any calculated force more than 7.9 N cannot be produced by the device[38]; therefore, cannot be truly perceived by the operator. Tuning the gains will allow us to ensure that all the forces (computed according to expected slave position errors) are producible by the haptic device. These gains were then kept constant for all experiments. Figure 7 further shows how the values of position error, operator's hand speed, and

task completion time changed when the impedance gains varied from 0 $\frac{N}{m}$ (force-disabled mode) to 300 $\frac{N}{m}$. As seen, increasing values of gains from 0 $\frac{N}{m}$ to 125 $\frac{N}{m}$ did not effectively change the position error. This was in line with our observation that the force generated was not large enough to allow the operator react to it accordingly. On the other hand, using values over 250 $\frac{N}{m}$ did not produce further improvement as the position error was close to E_{thr}. Therefore, the value of 250 $\frac{N}{m}$ was chosen to have the scheme tuned.

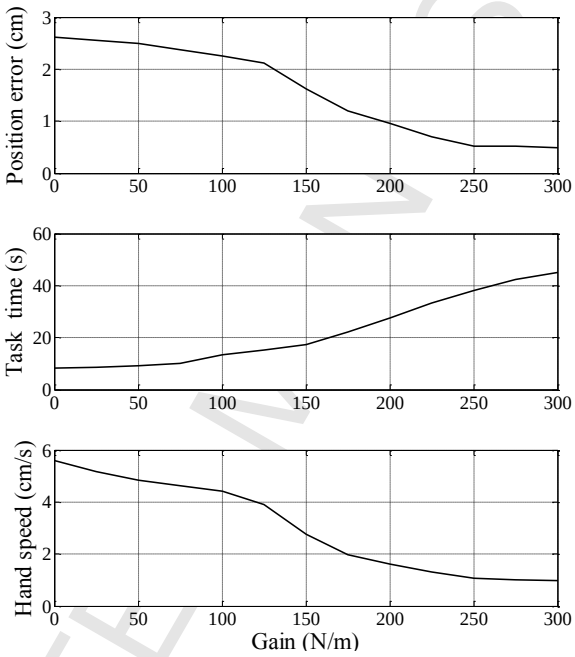

Figure 7. Mean values of slave position errors, task times and operator's hand speeds over different gains (diagonal elements of G), for scenario S1: TD=400 ms and PL=0%.

Results of two typical tests are presented: test in presence of a significant packet loss (TD=400 ms, PL=75%) and test in presence of a significant time delay (TD=1300 ms, PL=0%). Figure 8 shows typical master and slave trajectories with respect to frame $\{x_R y_R z_R\}$, when TD=400 ms and PL=75%. As shown, in haptic force-enabled mode, the actual position of the end-effector nearly overlaps with the desired position as compared to the case in which no force was applied to the operator's hand. Figure 9 illustrates variations of the radial position error ($\sqrt{e_x^2 + e_y^2 + e_z^2}$) at the slave end-effector, the operator's hand speed, and the haptic force applied to the operator's hand. As shown in haptic force-enabled mode, the more the position error is observed, the more the force will be produced. The average position error at the slave end-effector reduced from 3.06 cm (force-disabled) to 0.42 cm (force-enabled). Note that

E_{thr}=0.28 cm is the maximum radial steady-state error produced by the NPI controller. The average speeds in force-disabled and force-enabled tests were 4.23 $\frac{cm}{s}$ and 0.92 $\frac{cm}{s}$, respectively (see Figure 8).

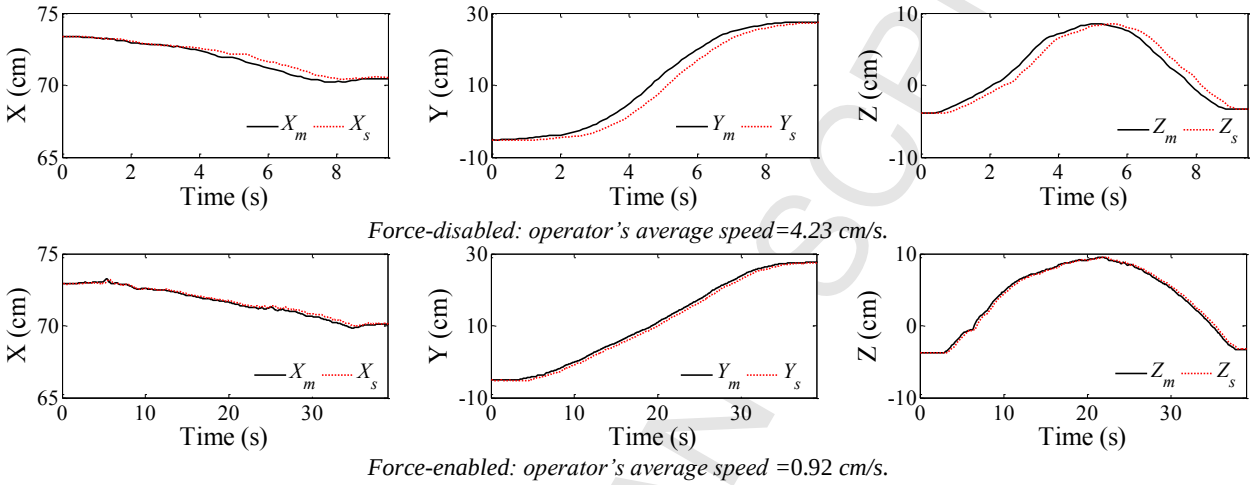

Force-disabled: operator's average speed=4.23 cm/s.

Force-enabled: operator's average speed =0.92 *cm/s.*

Figure 8. Hydraulic manipulator end-effector trajectory in frame $\{x_R y_R z_R\}$, for scenario S4: TD=400 ms and PL=75%. Subscripts 'm' and 's' indicate the displacement belongs to master or slave, respectively.

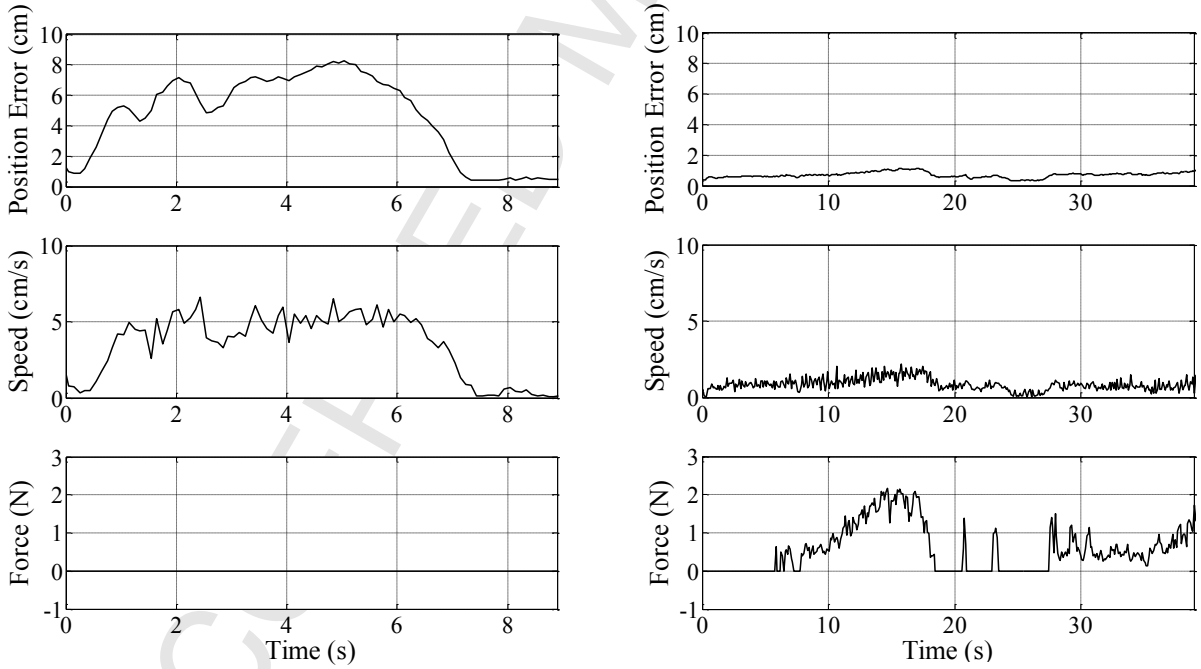

Force-disabled: average position error =3.06 *cm.* *Force-enabled: average position error* =0.42 *cm.*

Figure 9. Position error at the slave end-effector, operator's hand speed and haptic force, for test shown in Figure 8.

Typical position of the slave end-effector, when time delay is significant (TD=1300 ms and PL=0%) is shown in Figure 10. By comparing position signals of both modes, position error at the manipulator end-effector is observed to reduce when the position error-referenced force

scheme was included in the teleoperated system. In both scenarios, reduction of the hand's speed resulted in increasing the task completion time as expected.

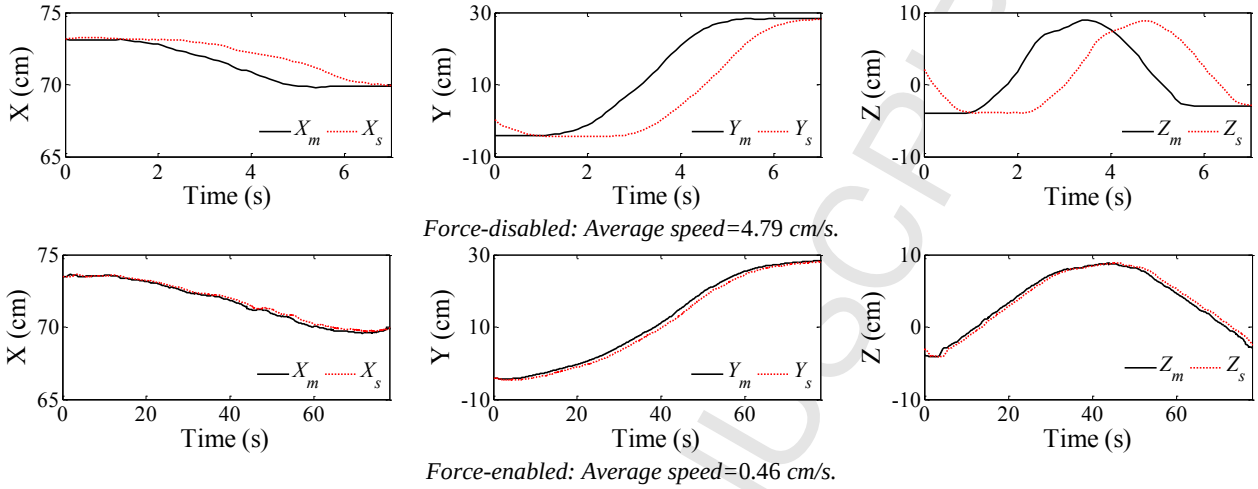

Force-disabled: Average speed=4.79 *cm/s.*

Force-enabled: Average speed=0.46 *cm/s.*

Figure 10. Hydraulic manipulator end-effector trajectory in frame $\{x_R y_R z_R\}$, for test S13 (TD=1300 ms; PL=0%).

Another test was performed with a large time delay and where the task was less monotonic, *i.e.*, the direction of motion was altered arbitrarily during the task. Figure 11 depicts the position of the slave end-effector for both force-disabled and force-enabled modes. As seen, the position error decreased (having a mean position error of 0.78 cm) when the control scheme was included in the system, as compared to the force-disabled mode with mean position error of 10.53 cm.

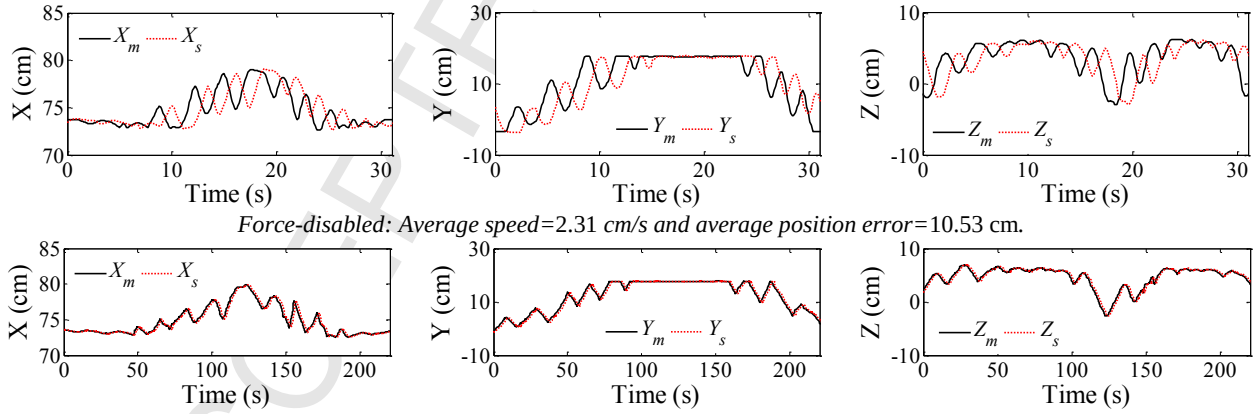

Force-disabled: Average speed=2.31 *cm/s and average position error*=10.53 cm.

Force-enabled: Average speed=0.34 *cm/s and average position error*=0.78 cm.

Figure 11. Manipulator end-effector trajectory in frame $\{x_R y_R z_R\}$, for a typical large time delay (TD=1300 ms) when the direction of the movement changes frequently.

5.2. Validation under wireless channel

In the second set of experiments, the effectiveness of the proposed scheme was evaluated in the presence of wireless channel emulated by the NS2 simulator. Different antenna transmission

powers, in obstructed and unobstructed environments, were emulated. Table 2 lists the important parameters used for test scenarios. In these tests, the wireless router was assumed to operate at 2.4 GHz with channel bandwidth of 11 $Mbps$. The antenna transmission power was set to 15 dBm (S17 and S19) and 18 dBm (S18 and S20) for low power and high power antennas, respectively. The receiver sensitivity was set to -83 dBm that is consistent with the receiver used in our setup. The path exponents, n was set to 2 dB (S19 and S20) and 3.5 dB (S17 and S18) to reflect unobstructed and obstructed environments, respectively. In all four experiments, the distance between the slave and the master sites was set to 50 m, which is a common distance that the live-line maintenance is practically performed.

Table 2. Parameters used to emulate wireless channel using NS2.

Parameter	Value
Path loss exponent	2 dB (unobstructed) 3.5 dB (obstructed)
Shadowing deviation	4.0 dB
Reference distance	1 m
Transmitting antenna gain	2 dBi
Receiving antenna gain	2 dBi
Antenna transmission power	15 dBm (low power) 18 dBm (high power)
Channel bandwidth	11 $Mbits/s$
Short retry limit	2
long retry limit	1
Packet size	50 $bits$
Packet interval	2 ms
Frequency	2.412 GHz
RTS Threshold	10000 (RTS/CTS disabled)
Carrier Sense Threshold	-83 dBm

Typical variations of packet loss and time delay over time, for scenarios S17 and S18, are shown in Figure 12. As expected, the packet loss randomly changes when the master and slave are connected wirelessly. Moreover, the packet loss for scenario S18 with high power is less than that with lower power (S17). Note that, the time delay was almost constant[39] and the packet loss was the dominant parameter in this set of experiments.

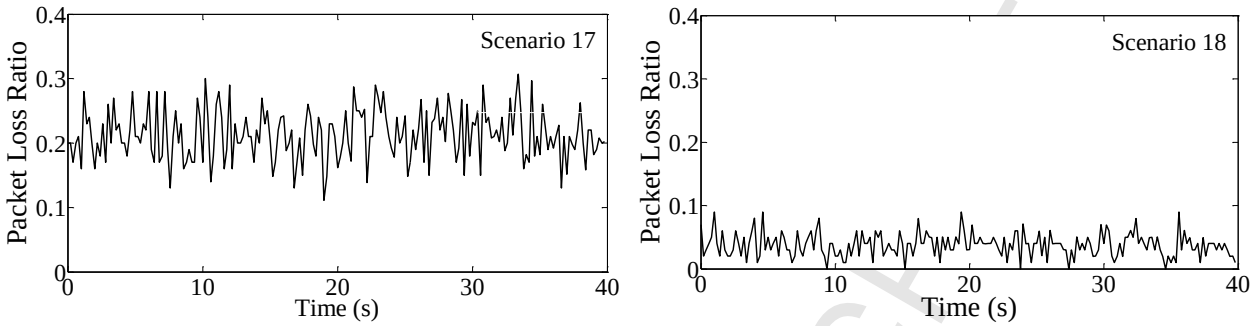

Figure 12. Typical packet loss generated in obstructed, low power antenna scenario (S17) and obstructed, high power antenna scenario (S18).

Figure 13 shows position tracking of the slave manipulator end-effector when the system operated in obstructed environment and a router with the antenna power of 15 dBm was used (scenario S17). When the force was activated, the operator moved the haptic device approximately four times slower than for the case it was deactivated. Figure 14 depicts similar results when the environment was obstructed, and a high power antenna (18 dBm) was employed (scenario S18). From Figures 13 and 14, it is observed that the position error at the end-effector decreased when the scheme was implemented in the system. More specifically, the average position error, for scenario S18, changed from 34.2 mm to 5.27 mm when the force slowed down the operator's hand motion. It was observed that regardless of router type and obstruction in the environment, the slave manipulator positioning improved when the haptic device utilized the proposed force to slow down the hand's motion.

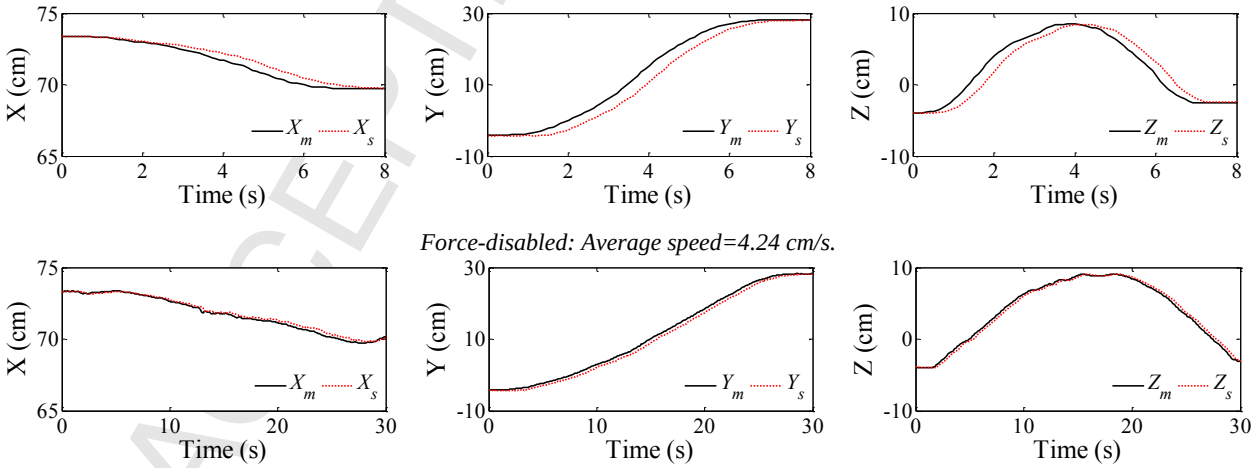

Figure 13. Slave end-effector trajectory in frame $\{x_R y_R z_R\}$, for scenario S17 emulating low power antenna and obstructed environment.

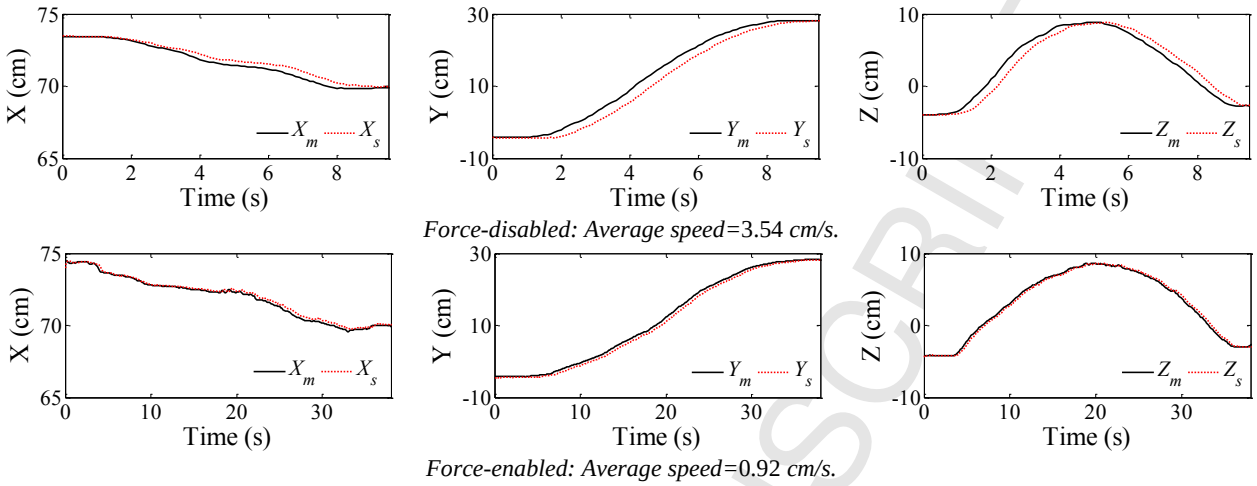

Figure 14. Manipulator end-effector trajectory in frame $\{x_R y_R z_R\}$, for scenario S18 (high power antenna and obstructed environment).

Figure 15 summarizes the information collected from all 400 trial runs: mean values of position errors, task completion times, and operator's hand speeds for all 20 scenarios. They were calculated by averaging the corresponding values that were measured each over 10 trials. As observed, in all 20 scenarios, the mean value of position error was significantly reduced when the haptic force was enabled. Specifically, the scheme reduced position error at the slave end-effector by at least 92%. This was done by simply slowing down the haptic motion guided by the force applied to the operator's hand. As a result, there was about four times increase in the task completion time when the proposed force augmentation scheme was included in the system. Figure 15 also depicts the mean values of the operator's hand speed which shows how the scheme reduces the hand's speed. P-values of position errors, task completion times, and hand speeds were 3.25×10^{-5}, 1.12×10^{-3}, and 7.805×10^{-3}, respectively, which show that all three indices were statistically significant.

Table 3 lists the mean vale and standard deviation (SD) of position errors at the slave manipulator end-effector, for each scenario. As observed, when the system operated under force-enabled mode, not only the mean value of slave position errors reduces, but also variation of the position errors around the mean value is smaller than the force-disabled mode.

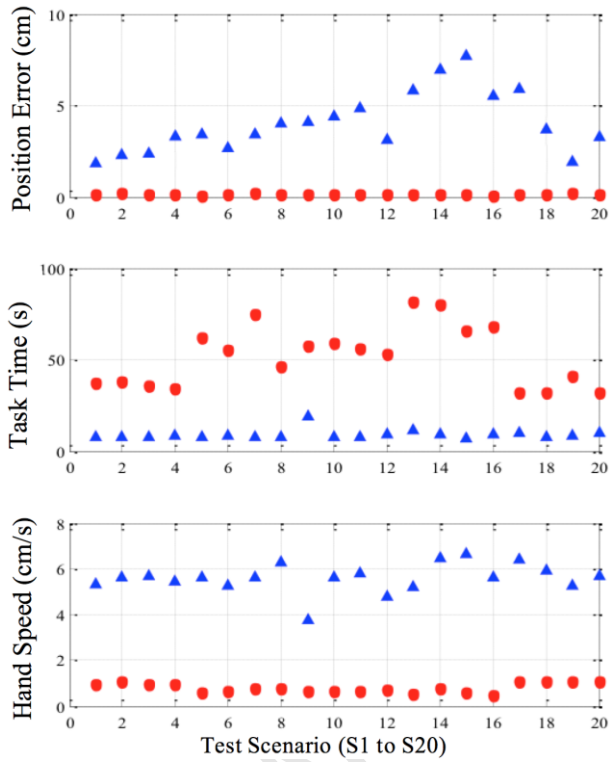

Figure 15. Mean values of position errors, task completion times, and operator's hand speeds without force (▲) and with force (●), for all 20 scenarios.

Table 3. Mean value±SD (in mm) of slave position errors for all 20 scenarios.

Force mode	**S1**	**S2**	**S3**	**S4**	**S5**	**S6**	**S7**	**S8**	**S9**	**S10**
Disabled	20.3±5.3	24.1±6.0	25.6±7.2	30.6±7.3	32.4±6.3	27.0±7.4	33.1±7.9	39.2±11.6	40.1±10.4	43.7±9.9
Enabled	4.0±0.1	4.8±0.1	4.6±0.1	4.2±0.1	4.9±0.1	4.7±0.1	5.4±0.2	7.3±0.3	6.9±0.2	5.1±0.2
	S11	**S12**	**S13**	**S14**	**S15**	**S16**	**S17**	**S18**	**S19**	**S20**
Disabled	46.9±13.5	31.3±6.1	55.8±18.6	68.1±16.0	77.1±25.6	53.5±12.9	55.6±17.5	34.2±7.7	21.3±6.2	33.9±6.5
Enabled	5.3±0.2	4.9±0.2	6.0±0.2	5.4±0.2	6.3±0.3	7.1±0.2	6.0±0.2	5.3±0.1	4.2±0.1	5.4±0.2

Analysis of Variance (ANOVA) test was conducted to test whether each network, scenario examined here, has a significant effect on the value of position error during the performance of each experiment. We analyzed the differences between mean values in force-enabled and force-disabled modes in each scenario. For all scenarios, the number of position error data was adequate to conduct a valid test. Table 4 lists the p-values obtained for each network scenario. P-values below 0.05 are considered significant[40]. As observed, the ANOVA test indicated that there was a significant difference in mean values of position errors, as all p-values were less than 0.05. Therefore, the type of network chosen can affect the value of the position error.

Table 4. P-values obtained using the ANOVA test.

Scenario	**S1**	**S2**	**S3**	**S4**	**S5**	**S6**	**S7**	**S8**	**S9**	**S10**
P-value	2.02×10^{-4}	6.00×10^{-3}	2.02×10^{-4}	8.88×10^{-5}	1.09×10^{-2}	5.79×10^{-5}	3.22×10^{-2}	4.91×10^{-7}	9.00×10^{-6}	3.23×10^{-3}
Scenario	**S11**	**S12**	**S13**	**S14**	**S15**	**S16**	**S17**	**S18**	**S19**	**S20**
P-value	4.01×10^{-8}	5.53×10^{-4}	8.66×10^{-7}	3.27×10^{-2}	3.24×10^{-3}	1.99×10^{-6}	2.02×10^{-4}	3.40×10^{-3}	7.43×10^{-3}	1.98×10^{-2}

Based on simulation and the experimental results, the proposed method works well under the network conditions found in outdoor live-line maintenance[41]. Practically, three safety measures were designed to prevent failures that include (*i*) continuously check network delay and jitter by sending probe packet from the slave site, if they are beyond thresholds, (*ii*) stop the slave manipulator immediately, and (*iii*) limit the motion range of the slave actuators.

5.3. Comparing proposed and conventional schemes

This section presents results of a set of experiment that was considered to compare the effectiveness of the proposed scheme and the conventional scheme. The operator was asked to perform a typical task to connect the lower joint of the insulator (see Figure 16), when the conventional slave position-referenced force was applied upon existence of position error at the slave end-effector. The test was then repeated when the proposed force was produced when the position error was observed. Note that in both forces, the magnitude of the force was proportional to the position error at the slave manipulator end-effector. However, in the proposed scheme this force was in the same direction as in the haptic device (operator's hand) current speed as opposed to the conventional force in which it is in the direction of the slave position error. In this study, in total, 2(schemes)×20(runs)=40 trials were collected for one operator. The scenario S2 (TD=400 *ms* and PL=25%) was emulated during this experiment.

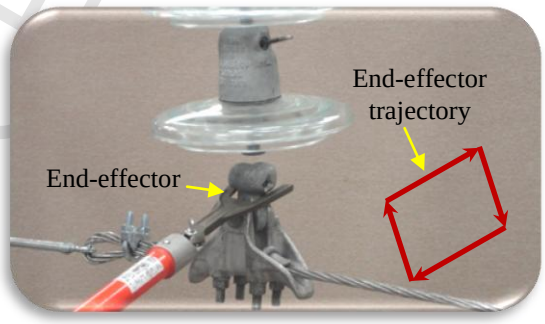

Figure 16. Typical task chosen to compare the conventional and the proposed schemes. The slave end-effector travels along a square path to connect the lower joint of the insulator.

Figure 17 illustrates mean values of position errors at slave end-effector and the operator's hand speeds, for all 40 trials: 20 trials with the conventional force (▲) and 20 trials with the proposed force (●). As observed in Figure 16, for this typical experiment, implementing the proposed force reduced the mean value of position errors by 72% compared to the conventional force (0.71 cm using the proposed scheme *vs.* 2.56 cm using the conventional scheme). However, in average, the operator was able to complete the tasks 25% slower under the proposed scheme (5.02 $\frac{cm}{s}$ in the proposed scheme *vs.* 6.74 $\frac{cm}{s}$ in the conventional scheme).

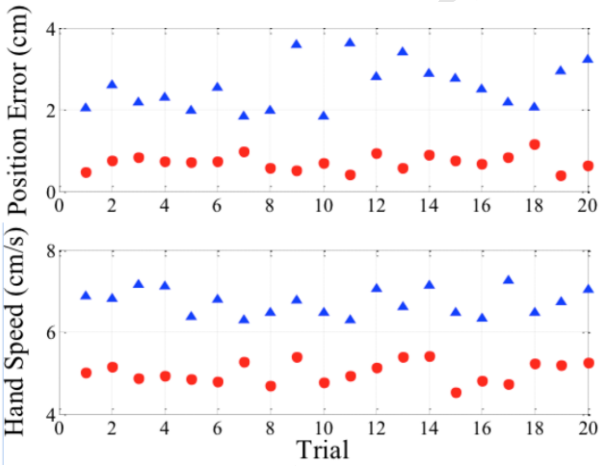

Figure 17. Mean values of position errors and operator's hand speeds with conventional force (▲) and with proposed force (●).

6. CONCLUSIONS

This paper presented a novel position error-referenced force scheme to reduce tracking errors, of a robotic manipulator that was controlled through a delayed and lossy communication channel. This scheme commands the haptic master device to apply a force against the operator's hand intended motion to slow down when position error is observed at the manipulator end-effector. Effectiveness of the scheme was evaluated by conducting experiments on a teleoperated hydraulic manipulator, when the system operated under different scenarios of dedicated and wireless communication channels. Results indicated that, for the tasks investigated in this paper, the proposed force scheme could reduce the position error at the slave hydraulic manipulator up to 92% as compared to the conventional system without force. Naturally, the task completion time increased when the haptic force guided the operator to reduce the hand's speed. Analysis of Variance (ANOVA) test was also conducted to test whether the chosen network scenario could have a significant effect on the value of position error. We detected significant differences

between the position errors in both force-enabled and force-disabled modes. Note that, in the proposed method, the amount of which the hand speed is to be slowed down is dictated based on the measured position error. Otherwise, without having knowledge about the values of time delay and packet loss, a lineman has to always move the device at the lowest possible speed which is inefficient compared to the condition in which our software decides on the speed based on the errors observed. Besides, the proposed method worked well with precision-oriented tasks in live-line maintenance such as grasping and then tightening/loosening a nut under the insulator or de-icing the power lines that requires a high accuracy (precision-oriented) while the speed and time of task completion are not crucial.

Overall, this paper, which is believed to make a further contribution to the development of feedback systems in telemanipulators, showed that the proposed scheme is practical, and can lead to positioning improvement, and should seriously be considered as a potential method for error improvement in teleoperated manipulators working under a delayed and lossy network in the field. Future work will focus on theoretical treatment of system stability to characterize the range of conditions in a teleoperated system as well as validating the proposed scheme under a real communication channel. Robustness of the proposed scheme for performing various tasks by different operators (novice and experienced) and over multiple trials by the same operator could also be studied in future. The authors are now extending the proposed scheme to orientation control, as many robot controllers have the same form of control law for both position and orientation control.

REFERENCES

[1] B. Zhang, T. S. Eugene Ng, A. Nandi, R. Riedi, P. Druschel, and G. Wang, "Measurement-based analysis, modeling, and synthesis of the Internet delay space, *IEEE/ACM Transactions on Networking*, vol. 18, no 1, pp. 229-242, 2010.

[2] Y. Maddahi, R. A. Rahman, W. K. Fung, and N. Sepehri, "Effect of network quality on performance of bilateral teleoperated hydraulic actuators: a comparative study," *Journal of Control and Intelligent Systems*, vol. 41, no. 1, pp. 11-25, 2013.

[3] A. Mohammadi, M. Tavakoli, H.J. Marquez, and F. Hashemzadeh, "Nonlinear disturbance observer design for robotic manipulators," *Journal of Control Engineering Practice*, vol. 21, issue 3, pp. 253-267, 2013.

[4] K. H. Suny, H. Momeni, and F. J. Sharifi, "Model reference adaptive control design for a teleoperation system with output prediction," *Journal of Intelligent and Robotic Systems*, vol. 59, issue 3-4, pp. 319-339, 2010.

[5] D. Chen, X. Tang, N. Xi, Y. Wang, and H. Li, "Stability analysis for Internet based teleoperated robot using prediction control," *IEEE International Conference on Cyber Technology in Automation, Control, and Intelligent Systems*, pp. 138-143, pp. 20-23, 2011.

[6] E. Kamrani, "Real-time Internet-based teleoperation," *Journal of Intelligent Control and Automation*, vol. 3, pp. 356-375, 2012.

[7] Kawashima, K.; Tadano, K.; Cong Wang; Sankaranarayanan, G.; Hannaford, B., "Bilateral teleoperation with time delay using modified wave variable based controller," *IEEE International Conference on Robotics and Automation*, pp. 4326-4331, 2009.

[8] S. Munir and W. Book, "Internet-based teleoperation using wave variable with prediction," *IEEE Trans. on Mechatronics*, vol. 7, no. 2, pp. 124-133, 2002.

[9] N.A. Tanner and G. Niemeyer, "Improving perception in time delayed teleoperation," *IEEE International Conference on Robotics and Automation*, pp. 354-359, 2005.

[10] N.A. Tanner, and G. Niemeyer, "High-frequency acceleration feedback in wave variable telerobotics," *IEEE/ASME Transactions on Mechatronics*, vol. 11, no. 2, pp. 119-127, 2006.

[11] C. Secchi, S. Stramigioli, and C. Fantuzzi, "Position drift compensation in port-Hamiltonian based telemanipulation," in *Proc. IEEE Int. Conf. on Intelligent Robots and Systems*, pp. 4211–4216, 2006.

[12] P. Arcara and C. Melchiorri, "Position drift compensation for a passivitybased telemanipulation control scheme," in *Proc. of Mechatronics Conference*, Enschede, The Netherlands, June 2002.

[13] E. J. Rodriguez-Seda, "Transparency compensation for bilateral teleoperators with communication time-varying delays," in *Proc. Int. Conf. on Intelligent Robots and Systems*, pp. 4375–4380, 2014.

[14] R. J. Anderson and M. W. Spong, "Bilateral control of teleoperators with time delay," in *Proc. IEEE Conf. Decision Control*, Austin, pp. 167–173, 1988.

[15] J. Kim, P.-H. Chang, and H.-S. Park, "Two-channel transparency optimized control architectures in bilateral teleoperation with time delay," *IEEE Trans. Control Syst. Technol.*, vol. 21, no. 1, pp. 40– 51, 2013.

[16] C. Secchi, S. Stramigioli, and C. Fantuzzi, "Position drift compensation in port-Hamiltonian based telemanipulation," *IEEE/RSJ Int. Conf. Intell. Robots Syst.*, Beijing, China, pp. 4211-4216, 2006.

[17] M. Franken, S. Stramigioli, S. Misra, C. Secchi, and A. Macchelli, "Bilateral telemanipulation with time delays: A two-layer approach combining passivity and transparency," *IEEE Trans. Robot.*, vol. 27, no. 4, pp. 741–756, 2011.

[18] E. J. Rodriguez-Seda and M. W. Spong, "A time-varying wave impedance approach for transparency compensation in bilateral teleoperation," in *Proc. IEEE/RSJ Int. Conf. Intell. Robots Syst.*, St. Louis, pp. 4609-4615, 2009.

[19] K. Hashtrudi-Zaad and S. E. Salcudean, "Analysis of control architectures for teleoperation systems with impedance/admittance master and slave manipulators," *Int. Journal of Robotics Research*, vol. 20, no. 6, pp. 419–445, 2001.

[20] E. J. Rodriguez-Seda, D. Lee, and M. W. Spong, "Experimental comparison study of control architectures for bilateral teleoperators," *IEEE Trans. on Robotics*, vol. 25, no. 6, pp. 1304-1318, 2009.

[21] K. Zarei-Nia, A.Y. Goharrizi, N. Sepehri, and W. K. Fung, "Experimental evaluation of bilateral control schemes applied to hydraulic actuators: a comparative study," *Transactions of the Canadian Society for Mechanical Engineering*, vol. 33, no. 3, pp. 377-398, 2009.

[22] G. Sankaranarayanan and B. Hannaford, "Experimental Internet haptic collaboration using virtual coupling schemes," in *Proc. Symposium on Haptic Interfaces for Virtual Environment and Teleoperator Systems*, USA, pp. 259-266, 2008.

[23] G. Sankaranarayanan and B. Hannaford, "Virtual coupling schemes for position coherency in networked haptic environments," in *Proc. of IEEE International Conference on Biomedical Robotics and Biomechatronics*, Italy, pp. 853 – 858, 2006.

[24] M. E. Kontz, M. C. Herrera, J. D. Huggins, and W. J. Book, "Impedance shaping for improved feel in hydraulic systems," in *Proc. ASME International Mechanical Engineering Congress and Exposition*, pp. 185-194, 2008.

[25] H. Hayn and D. Schwarzmann, "Control concept for a hydraulic mobile machine using a haptic operating device," in *Proc. International Conferences Advances in Computer-Human Interactions*, pp. 348-353, 2009.

[26] S. H. Ahn, H. S. Jung, Y. K. Kim, and H. R. Kim, "A compliance control for position referenced bilateral control systems," in *Proc. Int. Conf. on Intelligent Systems and Control*, pp. 49-53, USA, 2006.

[27] J. J. Abbott and A. M. Okamura, "Stable forbidden-region virtual fixtures for bilateral telemanipulation," *Journal of Dynamic Systems, Measurement and Control*, vol. 128, no. 3, pp. 53-64, 2006.

[28] A. Bettini, P. Marayong, S. Lang, A. M. Okamura, and G. D. Hager, "Vision-assisted control for manipulation using virtual fixtures," *IEEE Transactions on Robotics*, vol. 20, pp. 953-966, 2004.

[29] K. Zarei-nia, Y. Maddahi, N. Sepehri, T. Olson, and W. Mueller, "Unilateral control of teleoperated hydraulic manipulators applied to live line maintenance: Comparative study", *Journal of Robotics and Automation*, vol. 29, issue 2, pp. 162-174, 2014.

[30] C. A. Moore Jr., M. A. Peshkin, and J. E. Colgate, "Cobot implementation of virtual paths and 3-D virtual surfaces," *IEEE Trans. Rob. Autom.*, vol. 19, pp. 347-351, 2003.

[31] S.A. Bowyer, B. L. Davies, and F. Rodriguez y Baena, "Active constraints/virtual fixtures: a Survey," IEEE Trans. on Robotics, vol. 30, issue 1, pp. 138-157, 2014.

[32] P. Marayong, A. Bettini, and A. Okamura, "Effect of virtual fixture compliance on human-machine cooperative manipulation," in *Proc. IEEE/RSJ Int. Conf. on Intelligent Robots and Systems*, pp. 1089-1095, 2002.

[33] Y. Maddahi, K. Zarei-nia, and N. Sepehri, "An augmented virtual fixture to improve task performance in robot-assisted live-line maintenance," *Journal of Computers and Electrical Engineering*, vol. 43, pp. 292-305, 2015.

[34] Y. Maddahi, K. Zareinia, N. Sepehri, T. Olson, and W. Mueller, "Live-line maintenance training using robotics technology", *IEEE World Haptics Conf.*, Korea, pp. 587-592, 2013.

[35] N. Sepehri, A. A. Khayyat, and B. Heinrichs, "Development of a nonlinear PI controller for accurate positioning of an industrial hydraulic manipulator, " *Journal of Mechatronics*, vol. 7, pp. 683-700, 1997.

[36] T. Issariyakul and E. Hossain, "Introduction to network simulator NS2," Springer, 2009.

[37] T. Rappaport, "Wireless communications: principles and practice," *Prentice Hall*, 2002.

[38] K. Zareinia, Y. Maddahi, C. Ng, N. Sepehri, and G. R. Sutherland, "Performance evaluation of haptic hand-controllers in a robot-assisted surgical system," *Int J Med Robotics Comput Assist Surg*, DOI: 10.1002/rcs.1637, pp. 1-19.

[39] Y. Maddahi, N. Sepehri, S. Liao, W. K. Fung, and E. Hossain, "Wireless control of a teleoperated hydraulic manipulator with application towards live-line maintenance," *Proceedings of ASME/BATH Symposium on Fluid Power and Motion Control*, USA, p. 9, 2013.

[40] L. B. Rosenberg, "Virtual haptic overlays enhance performance in telepresence tasks," H. Das (Ed.), *Photonics for Industrial Applications*, vol. 2351, pp. 99–108, 1995.

[41] Y. Maddahi, S. Liao, W. K. Fung, E. Hossain, and N. Sepehri, "Selection of network parameters in wireless control of bilateral teleoperated manipulators," *IEEE Trans. on Industrial Informatic*s, doi: 10.1109/TII.2015.2490625, 2015.

***Biography of each author**

Yaser Maddahi received his B.Sc. and M.Sc. from Iran, in 2001 and 2003, respectively. Currently, he is a Graduate Research Fellow in the Mechanical Engineering at the University of Manitoba, Canada. He became member of IEEE, ASME, and CSME in 2009.
He was a lecturer and the head of Robotics and Automation Research Laboratory at the Islamic Azad University (Saveh branch) in Iran. His research interests include networked robotics, control of teleoperation systems, hydraulic telemanipulators, haptics, design of feedback control systems, and calibration of mobile robots.

Stephen Liao received his B.Sc. degree and M.Sc. degree in Computer Engineering from the University of Manitoba in 2009 and 2013, respectively. He became a member of IEEE in 2009. His research interests include networked robotics and image processing.

Wai-keung Fung received the B. Eng. degree in electronic engineering, the M. Phil degree in system engineering and engineering management, and the PhD degree in automation and computer aided engineering from the Chinese University of Hong Kong, Hong Kong, in 1994, 1996 and 2001, respectively. He was a postdoctoral research associate with the Department of Electrical and Computer Engineering, Michigan State University, East Lansing, Michigan, USA in 2001-2002 and a postdoctoral fellow with the Department of Automation and Computer Engineering, The Chinese University of Hong Kong in 2003-2005. He was assistant professor at Department of Electrical and Computer Engineering, University of Manitoba, Winnipeg, Manitoba, Canada in2005-2012.his research interest include Networked Robotics, Intelligent Robotics, Computational Intelligence, and Human-Machine Interaction. He has been IEEE Senior Member since 2009.

Nariman Sepehri is a professor with the Department of Mechanical Engineering, at the University of Manitoba, Canada. He received M.Sc. and Ph.D. degrees from the University of British Columbia, Canada. His research and development activities are primarily centered in all fluid power related aspects of systems, manipulation, diagnosis and control.

***Photo of each author**

Y. Maddahi

W-K Fung

S. Liao

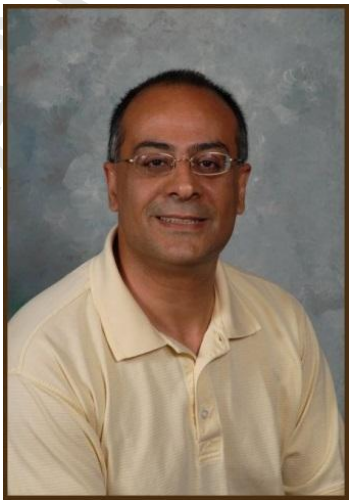

N. Sepehri